JOURNAL OF MATERIALS SCIENCE 18 (1983) 457–470

Microstructural development of sub-eutectoid aged $MgO–ZrO_2$ alloys

R. H. J. HANNINK
CSIRO, Division of Materials Science, Advanced Materials Laboratory, P.O. Box 4331, Melbourne, Victoria, Australia 3001

The microstructural development in fully and partially stabilized $MgO–ZrO_2$ alloys during sub-eutectoid heat treatment at 1100° C, has been studied by optical and electron microscopy and powder X-ray diffraction in order to correlate the observed microstructures with the mechanical properties. The materials used were 14 mol % $MgO–ZrO_2$ (Mg-CSZ) of eutectoid composition and 9 mol % $MgO–ZrO_2$ (Mg-PSZ). In Mg-CSZ the decomposition reaction proceeds almost to completion before the maximum thermal up-shock properties are attained. For the Mg–PSZ material the most significant event leading to the enhanced mechanical properties appears to be the nucleation and growth of a long-range ordered anion vacancy phase within the cubic zirconia matrix. This, in turn, leads to the destabilization of the tetragonal ZrO_2 precipitates also present in Mg-PSZ, causing some of them to acquire monoclinic intergrowths whilst others transform to the monoclinic form on cooling. Beyond about 4 h ageing at 1100° C the decomposition product in the grain boundaries began to influence the mechanical properties.

1. Introduction

Zirconia alloys have recently become the subject of wide-ranging investigations because they are considered to constitute a new class of strong/tough ceramics [1]. This interest stems from the ability of these alloys (and other systems containing zirconia dispersions) to develop improved mechanical properties as a result of a controlled phase transformation about the tip of a crack ([2–4], see also Heuer in [1]).

The toughening in partially stabilized zirconia alloys (PSZ) is achieved by careful control of the microstructure and phase distribution. PSZ alloys consist of grains with a cubic, c, stabilized zirconia matrix (CSZ), in which are dispersed small precipitates of tetragonal, t, and/or monoclinic, m, zirconia. The solute stabilizing the cubic phase is usually MgO, CaO, Y_2O_3 or a rare earth oxide. In peak strength PSZ most of the precipitates are t and have been developed (aged) to a size where they will spontaneously transform (via a martensitic reaction) to the room-temperature stable m form, under the influence of the stress field about a propagating crack. The t → m transformation is accompanied by volumetric dilation and shear which results in an enhanced fracture toughness. Zirconia alloys which exhibit this type of toughening are referred to as transformation toughened zirconia (TTZ).

The TTZ mechanism is not restricted to PSZ. The t → m transformation has been used to strengthen/toughen other ceramic systems, such as $Al_2O_3–ZrO_2$ and $SiN–ZrO_2$ [5, 6].

Magnesia-PSZ (Mg-PSZ) in the composition range 8 to 9 mol % MgO has been the most studied system to date [3, 7, 8]. In this system (see Fig. 1) the accepted method of producing TTZ material consists of a solution treatment in the single-phase c field, ~ 1750° C for commercial alloys, a rapid cool to room temperature and a subsequent ageing treatment above 1400° C. The ageing treatment above 1400° C coarsens the precipitated t particles to a size where they will transform in the stress field of a crack. The optimum size is about 0.2 μm in their longest dimension [3, 10]. In uncontrolled slow cooling or in extended ageing above 1400° C, the t precipitates grow to a size where they become semi- or incoherent with the

0022–2461/83/020457–14$04.18/0

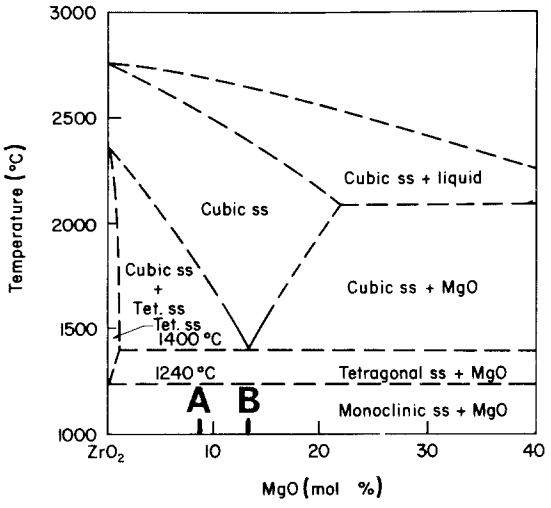

Figure 1 ZrO_2-rich end of the ZrO_2–MgO equilibrium phase diagram, after Grain [9]. Alloys examined in this investigation are indicated at (A) 9 mol% MgO, Mg-PSZ and (B) 14 mol% MgO, Mg-CSZ.

c matrix [3, 10]. When such a material is cooled to room temperature the precipitates transform spontaneously to m at about 1200° C and so lose the ability to significantly toughen the material.

It has been stated previously [12] that for Mg-PSZ that optimum mechanical properties are obtained by ageing at temperatures between 1400 and 1500° C. This temperature range was suggested because Mg-PSZ undergoes a eutectoid decomposition reaction below 1400° C and so heat treatments below this temperature are to be avoided [11, 12].

Few studies have been reported which examine the eutectoid decomposition of Mg-PSZ [11–14]. Viechnicki and Stubican [13] have examined the decomposition of hyper-eutectoid MgO–ZrO_2 systems whilst Porter and Heuer [12] have reported their observations on a rapidly cooled 8.1 mol% MgO–ZrO_2 hypo-eutectoid alloy. Both groups of investigators agree that the decomposition will follow a reaction suggested by the phase diagram shown in Fig. 1, namely:

$$\text{ageing} \geqslant 1200^\circ\text{C}, \text{CSZ} \rightarrow \text{t } ZrO_2 + \text{MgO}$$

$$\text{cool} \rightarrow \text{m } ZrO_2 + \text{MgO}$$

while ageing $\leqslant 1200^\circ$ C, CSZ $\rightarrow$ m ZrO_2 + MgO.

We have recently found that with a suitably pre-fired Mg-PSZ material, containing t precipitates of $\gtrsim 100$ nm in their longest dimension, further improvements in the mechanical properties can be obtained by ageing at 1100° C [15, 16]. The most significantly improved mechanical property is that measured by a fracture toughness test, where optimally aged material displays increased fracture energy and stable crack propagation (*R*-curve behaviour) [17]. In practical terms, the improved mechanical properties are demonstrated in a thermal up-shock test. This test is used to determine the probable industrial performance of zirconia materials [16]. The decomposition reaction has little detrimental effect on the mechanical properties of the material for the ageing times required to achieve the enhanced industrial performance.

A summary of recently reported room-temperature modulus of rupture (MOR) data for two sub-eutectoid aged (1100° C) MgO–ZrO_2 alloys of the present work is shown in Fig. 2 [15, 16, 18]. The initial difference in MOR between the two alloys is due to the fine dispersion of precipitates in the Mg-PSZ material [4]. From Fig. 2 it can be seen that in 14 mol% Mg-CSZ the MOR decreased rapidly during the first 2 h of ageing, and thereafter the MOR increased until a steady

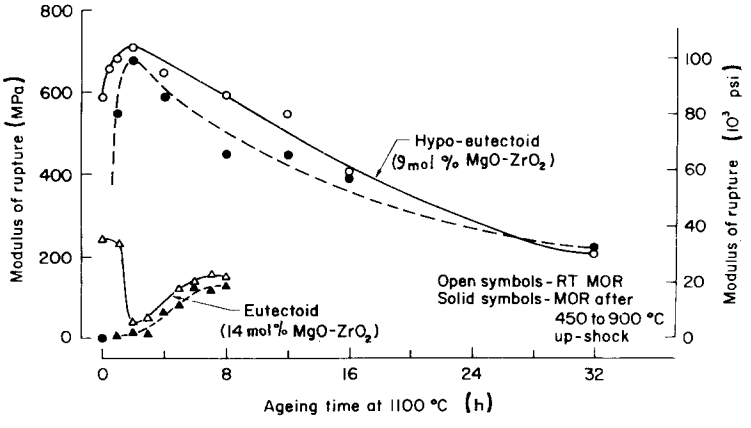

Figure 2 Modulus of rupture (MOR) data for two MgO–ZrO_2 alloys comparing the room-temperature MOR before and after thermal up-shock as a function of ageing time at 1100° C. 1 psi $\equiv 6.89 \times 10^3$ N m^{-2}.

TABLE I Lattice parameters of the c- and t-phases after ageing at 1100° C

Ageing time (h)	Cubic phase			Tetragonal phase		
	a_0 (Å)	Cell volume (Å^3)	% MgO	a (Å)	c (Å)	Cell volume (Å^3)
CSZ as-fired	5.0770 ± 0.0002	130.9	14.3	Not detected		
2	5.0771 ± 0.0002	130.9	14.3	Not detected		
PSZ as-fired	5.0801 ± 0.0018	131.1	13.3	5.0763 ± 0.0010	5.1804 ± 0.0017	133.5
0.5	5.0809 ± 0.0014	131.2	13.1	5.0777 ± 0.0014	5.1813 ± 0.0022	133.6
10	5.0783 ± 0.0041	131.0	13.9	5.0793 ± 0.0014	5.1827 ± 0.0025	133.7
32	5.0784 ± 0.0039	131.0	13.9	5.0809 ± 0.0037	5.1807 ± 0.0060	133.7

value was attained at about 8 h. The 9 mol% Mg-PSZ material, on the other hand, showed an increase in the MOR over the first 3 h ageing period. After this time the Mg-PSZ material passed the peak aged condition and gradually reduced in strength until beyond 32 h the strength was comparable to that of the Mg-CSZ materials. In both alloys some sub-eutectoid ageing was required before substantial strength could be retained after thermal up-shock.

The purpose of the present paper is to describe the microstructures which result from 1100° C ageing of the 14 mol% Mg-CSZ and 9 mol% Mg-PSZ alloys whose mechanical properties are summarized in Fig. 2. The sub-eutectoid ageing temperature of 1100° C was selected on an empirical basis. Our earlier investigations have shown that by ageing at 1100° C (i.e. in the m ZrO_2 + MgO-phase field of Fig. 1) the mechanical properties could be optimized and the thermal processes most readily controlled [15].

2. Experimental details

The eutectoid composition 14 mol% MgO–ZrO_2 and hypo-eutectoid 9 mol% MgO–ZrO_2 alloys were prepared by a previously reported method [15].

After firing at 1700° C the Mg-CSZ and Mg-PSZ materials were cooled at an average rate of 275° C h^{-1} to 1000° C and thereafter cooled at 70° C h^{-1} to room temperature. Both materials were subsequently reheated to 1100° C in air using an electric furnace and aged for the times indicated.

The mechanical testing techniques have been reported elsewhere [8], and the results are summarized in Fig. 2. Mechanically tested specimens were sectioned, mounted and polished prior to examination in an optical microscope or were ground, mechanically polished and thinned by Ar-ion bombardment for examination in a 200 kV electron microscope. Etching for optical microscopy was carried out in an HF bath at room temperature.

Lattice parameter measurements were determined from powder X-ray diffraction photographs taken with a Guinier camera. Both Ar-ion thinned foils and crushed samples were used as specimens. Thoria (a_0 = 5.5972 Å) was deposited on the foils or mixed with the crushed powder as an internal standard [10].

3. X-ray measurements

Lattice parameters of the c and t-phases, as determined from the Guinier photographs are shown in Table I. These values do not allow specific conclusions to be made concerning compositional variations as a function of ageing time, because the widths of the diffraction lines also increased with ageing time, causing a corresponding increase in the experimental standard deviations of the determined parameter. The X-ray line-broadening is attributed to matrix strain. Only lines due to c and m were observed in X-ray diffraction patterns of the Mg-CSZ materials. X-ray lines from Mg-CSZ specimens aged at times greater than 2 h, were so diffuse that meaningful measurements were not possible.

Although the standard deviations were large the actual determined lattice parameters for c appear

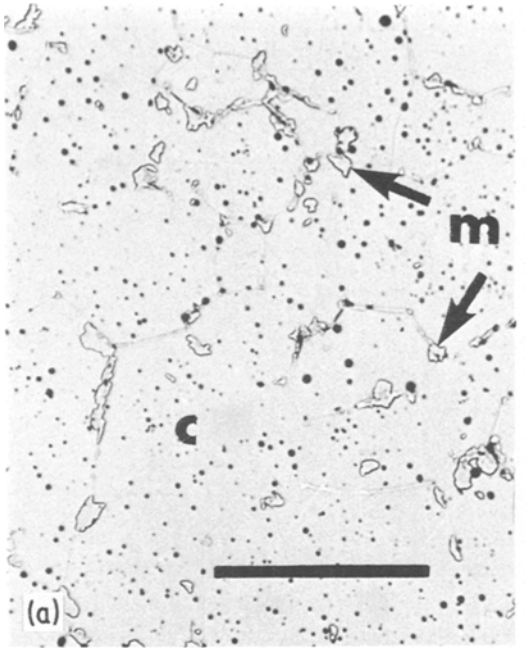

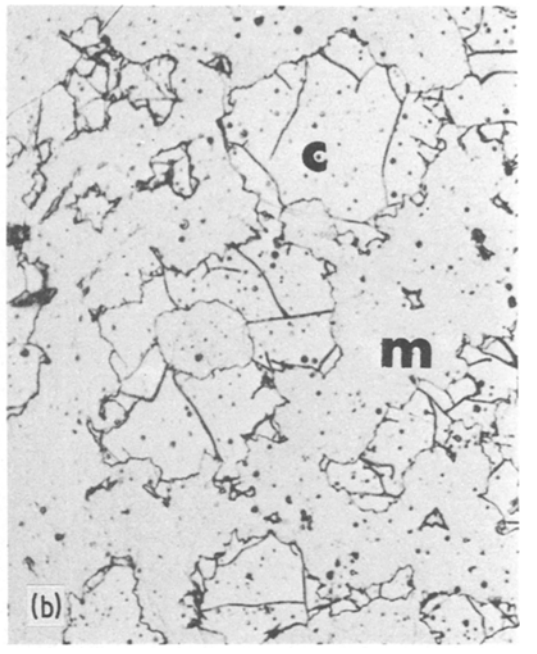

Figure 3 Optical micrographs of Mg-CSZ showing the c- and m-phases after ageing for (a) 1 h, (b) 3 h, and (c) 7 h at 1100° C. Note in (b) the severe cracking of the c-phase. Bar length equal 100 μm, all images at same magnification.

to decrease with time whilst those for t show a marginal increase. It is tempting to suggest that the lattice parameter variations might be an indication of matrix MgO diffusion. The consequences of this possible MgO segregation are further dealt with in Section 6.

The molar concentration of MgO (X_m) in c-matrix solid solutions, within the range 10 to 15 mol% can be determined from the c-lattice parameter, a_0 Å, by using the following relationship [19];

$$a_0 = 5.1220 - 0.3140X_m. \quad (1)$$

From the determinations of a_0 it is found that the Mg-CSZ material contained 14.3 mol% MgO, whilst the cubic phase of the Mg-PSZ matrix contained about 13.6 mol% MgO.

Magnesia or superlattice lines where not detected in the X-ray photographs from any of the aged samples. A separate study has shown that concentrations of at least 5 mol% are required before MgO can be detected as a separate phase [19].

4. Optical microscopy

Both of the as-fired materials consisted of a single-phase polycrystalline matrix, ~ 60 μm grain size, containing a uniform distribution of pores. After heating the Mg-CXZ material for ~ 1 h at 1100° C an m grain-boundary (GB) phase, resulting from the decomposition process, was evident (Fig. 3a). After 3 to 4 h heating the c-phase became the minor phase (Fig. 3b). It was severely cracked, as a result of thermal expansion differences between the c and m-phases, explaining the catastrophic reduction in MOR for the 2 to 4 h

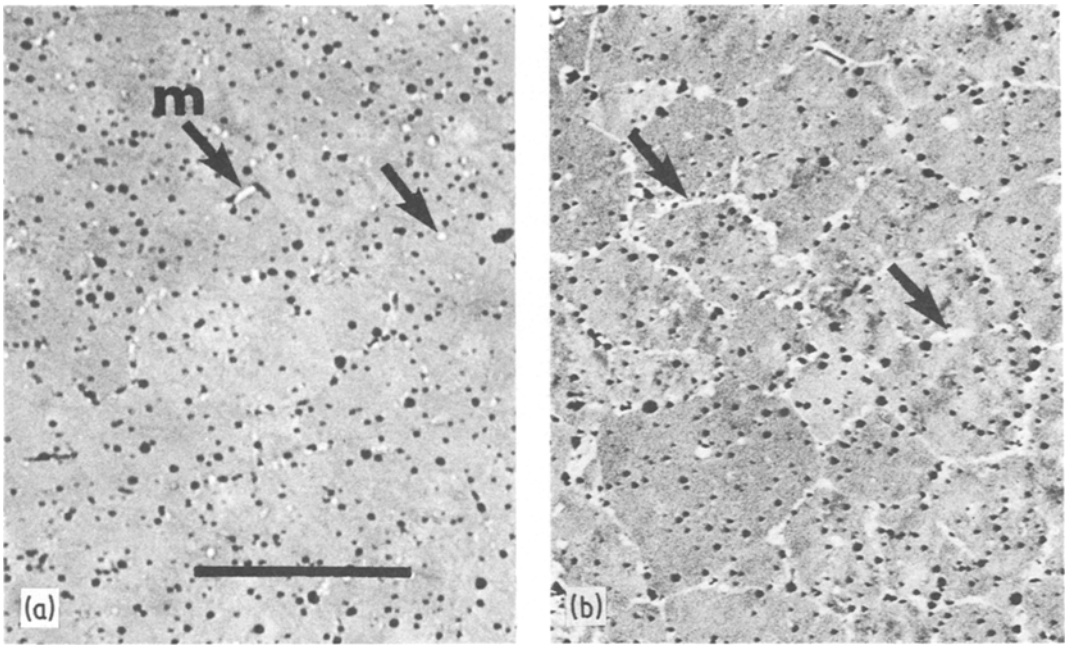

Figure 4 Optical micrography of Mg-PSZ; (a) as-fired material, (b) after ageing at 1100° C for 4 h, and (c) 32 h. Arrows indicate presence of m-phase. Bar length equals 100 μm, all images at same magnification.

aged material (see Fig. 2). After 6 h heating the c-phase had been reduced to well-dispersed islands and at 7 h the total c-phase content was about 5%, with the matrix now consisting of polycrystalline m (Fig. 3c). As seen from Fig. 2 this microstructure was responsible for the recovery of the MOR. The rate of the disappearance of the c-phase was similar to that observed by Viechniki and Stubican [13] for 20 mol% material aged at 1075° C, namely 90% decomposition after 4 h.

Ageing the Mg-PSZ alloy resulted only in a small initial change in the optical microstructure, until at 4 h ageing, the material just attained a continuous GB m-phase (cf. Fig. 4a and b). The presence of this phase did not result in any marked variation in the room-temperature MOR. Longer ageing times resulted in a continual increase in the GB m content and at 32 h the GB phase had consumed about 20% of the original grain diameter (Fig. 4c).

Beyond 32 h ageing, the room temperature mechanical properties of the Mg-PSZ material were so poor that further ageing was not pursued. From Fig. 2 it can be seen that for ageing times of 32 h and beyond, the GB phase controls the mechanical properties of the Mg-PSZ material: they are now very similar to those of the fully decomposed Mg-CSZ.

5. Electron microscopy of Mg-CSZ (TEM)

5.1. Microstructure of as-fired material

The grain interiors of the as-fired Mg-CSZ material consisted of a c-matrix and contained a dispersion of very fine precipitates. Fig. 5a shows the CSZ matrix with precipitate contrast in the extinction contour. Fig. 5b is the selected-area $[1\,2\,3]_c$ diffraction pattern (SAD) from the same region. In this

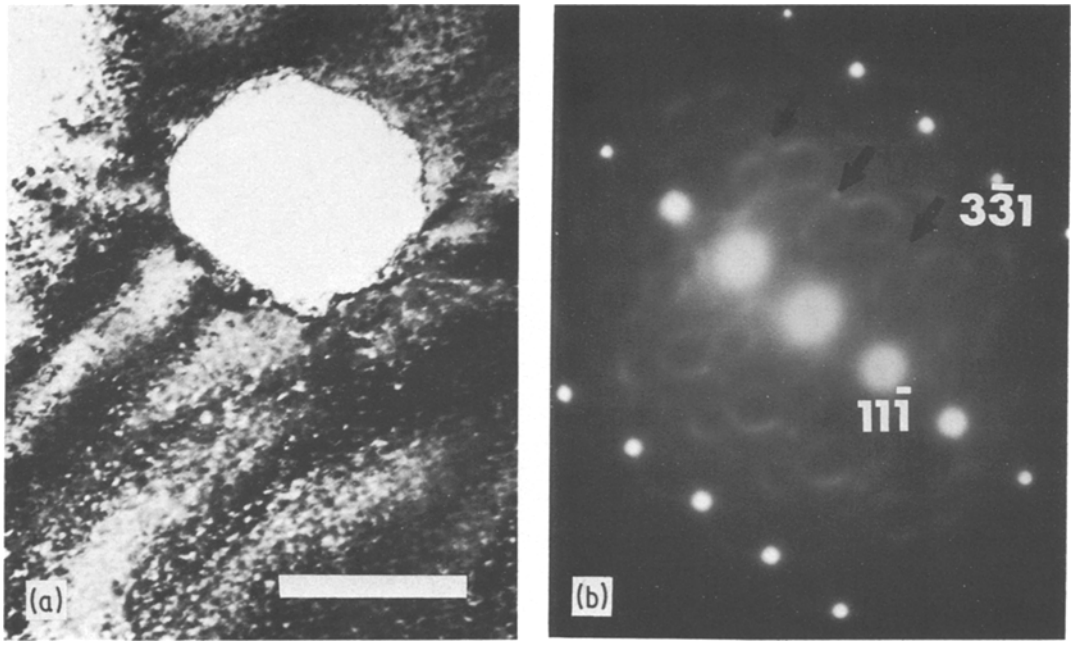

Figure 5 As fired Mg-CSZ material: (a) bright-field TEM of very small matrix precipitates; (b) selected-area electron diffraction pattern, $[123]_c$, of same area as (a), showing diffuse banding. Note also half order t reflections (arrowed) resulting from small t matrix precipitates. Bar length equals 0.5 μm.

pattern diffuse banding and half-order 220 diffraction spots are also visible. Using dark-field (DF) imaging techniques it was found that the diffuse banding arose from the matrix whilst the half-order spots came from the very fine matrix precipitates.

The diffuse banding has been interpreted as being due to micro-domains, ~3 nm diameter, of the fluorite-related superstructure δ-phase, $Mg_2Zr_5O_{12}$, coherent with the c matrix [20]. The half-order spots correspond to a t-phase, which is homogeneously nucleated and present as either spheres or discs with their largest dimension being ~15 nm. The presence of small t precipitates in a fully stabilized material appears to be out of place. Since the X-ray lattice parameter measurements of this sample suggest that it was of correct eutectoid composition, the presence of the t precipitates must be due to a cooling rate from the solution temperature that was slow enough to allow limited decomposition to occur below 1400° C. Resulting in homogeneous nucleation and precipitation of the t-phase.

This explanation is reinforced by the fact that some of the grain boundaries contained islands of m suggesting that decomposition had been nucleated during cooling from the solution temperature.

5.2. Effect of ageing on grain interiors

Ageing for 2 h at 1100° C increased the tetragonal precipitate size to about 30 nm, whilst not altering the banding configurations observed in SAD patterns. Diffraction contrast studies of the precipitates showed them to be small discs lying on {1 00} of the matrix. The discs exhibited the classical "line of no contrast" that occurs in the two beam diffraction situations when the diffraction vector, g, is normal to the zero displacement vector, R [21]. Fig. 6a to c show an area in which the same precipitates were examined using various values of g in the [001] section. From these images it can be seen that one set of precipitates was out of contrast in $g = 020$ or 200 whilst the other exhibited the line of no contrast. For $g = 220$ both sets of precipitates exhibited contrast. Precipitates lying on (001) were not visible when using the [001] section, since the lattice dilation was normal to the imaging beam, i.e. the product $g \cdot R = 0$.

After 4 h ageing the tetragonal precipitates in the remaining undecomposed cubic regions had grown in their longest dimension to 50 nm. As observed from optical micrographs very little cubic phase remained. The t precipitates attained a maximum size of about 50 nm before being con-

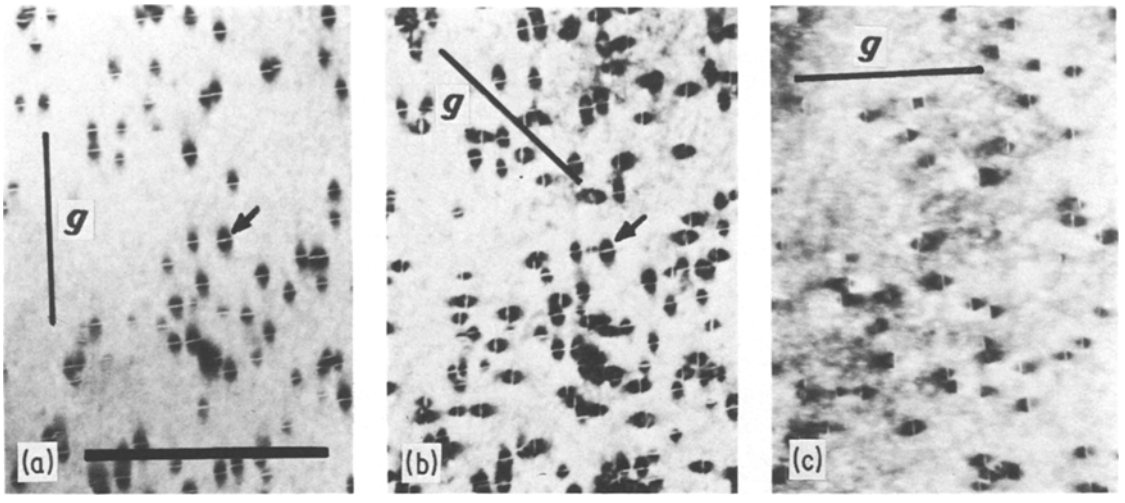

Figure 6 Tetragonal precipitates in Mg-CSZ matrix after 2 h ageing at 1100° C. Bright-field TEM images obtained using various two-beam diffraction conditions to illustrate in–out contrast of disc-shaped precipitates: (a) $g = 020$, (b) $g = \bar{2}20$, and (c) $g = 200$. Bar length equals 0.5 μm.

sumed by the decomposition processes, advancing as a front into the grain interior (cf. Fig. 3). SAD patterns of the 4 h aged material showed that the δ-phase, whilst still present in the matrix, was still there only as micro-domains.

5.3. Effect of ageing on grain boundaries

After 1 h, as seen in the optical micrographs, a considerable amount of eutectoid decomposition was present in the grain-boundary regions. A typical decomposed grain-boundary region, after 2 h ageing, is shown in Fig. 7a. The decomposition product occurred predominantly as continuous pipes. Energy-dispersive X-ray analysis (EDA) showed the pipes to be rich in magnesium. It should be recalled here, whilst EDA indicated

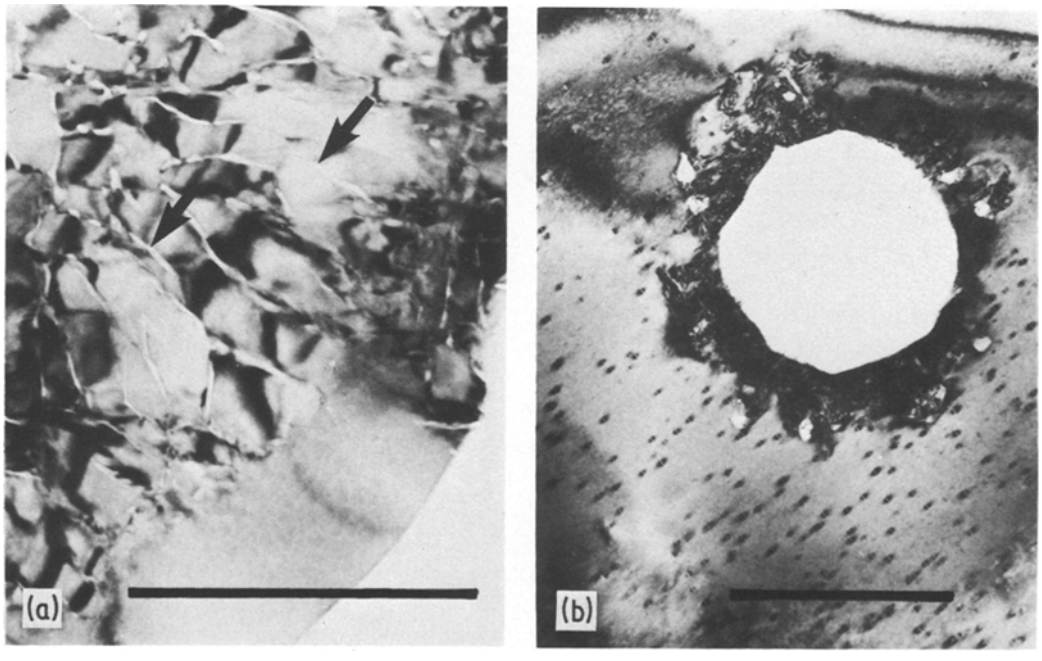

Figure 7 Bright-field TEM images showing the nucleation and growth of the decomposition products in Mg-CSZ. (a) Grain-boundary decomposition showing MgO-rich pipes (examples arrowed) separating m sub-grain regions within the same m grain, and (b) nucleation and growth from a pore. Bar length equals 1.0 μm.

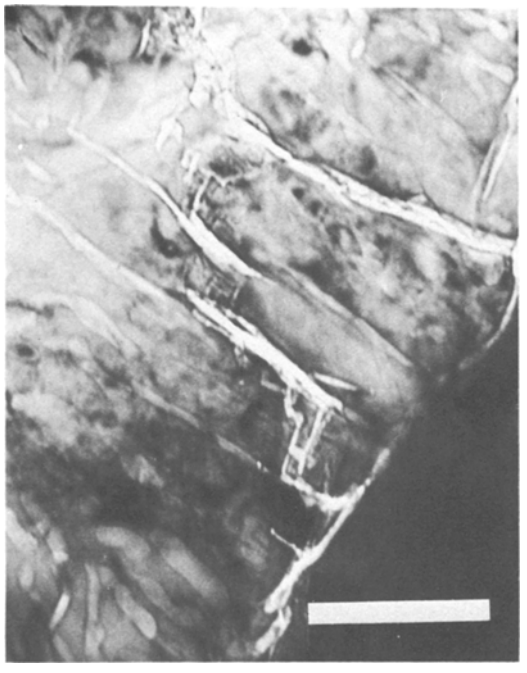

Figure 8 Crack in a decomposed region in Mg-CSZ. Note the copious crack–matrix/pipe interaction. Bar length equals 0.25 μm.

Mg-rich regions, X-ray diffraction failed either to show a significant increase in cubic matrix lattice parameter a_0, which would be expected on exsolution of MgO or to reveal the presence of MgO in the sample. As suggested by the extinction contours, the regions between the pipes were of a slightly different orientation, this observation indicates that the pipes formed the boundaries between polygonized regions or sub-grains of m. The m sub-grain size was about 0.1 μm whilst the monoclinic grain size was $\sim$ 2.5 μm. Fig. 7b shows that the decomposition process also begins about pores.

Examination of the decomposed areas revealed considerable microcrack networks, resulting from thermal expansion differences between the various orientations of m [22]. Fig. 8 is an image of a crack passing through a decomposed region and shows the extensive crack-pipe interaction.

5.4. Role of microstructure on mechanical properties

As reported elsewhere [17, 18], materials exhibiting extensive eutectoidally decomposed regions exhibit stable crack propagation and R-curve behaviour. The main contributors to the improved thermal shock behaviour in the present material is a consequence of the interaction between cracks and the decomposed matrix as seen in Fig. 8, and the lower thermal expansion coefficient of the m-phase [18]. This type of crack–matrix interaction has beneficial effects in terms of microcrack networks which result in a very high work of fracture. The direct result of the microcracks and hence very high work of fracture, coupled with the reduced thermal expansion coefficient, is seen here in the high fracture of retained MOR after the thermal up-shock test (Fig. 2).

Whilst the cubic matrix does contain t precipitates (Fig. 6), which grows to a maximum size of about 50 nm in 4 h, the precipitates do not influence the strength/toughness of the material. As shown in Fig. 3b, the presence of the crack network in the c-phase will control the MOR at short ageing times, so that the presence of the c-phase, containing the t precipitates, tends to decrease the fracture strength (Fig. 2).

6. Electron microscopy of Mg-PSZ

6.1. Microstructure of as-fired material

The as-fired PSZ material employed in this investigation consisted of a c-stabilized matrix containing t precipitates whose longest dimension was $\sim$ 160 nm. This type of microstructure is now well known and is generally considered to be that required for a near peak-strength material [3, 8]. SAD patterns of such a material showed the typical c and t diffraction spots. Very careful examination of a number of SAD patterns also showed weak diffuse banding and very weak m diffraction spots. The m diffraction spots arose from formally large t precipitates which had transformed to a very fine network of (1 1 0) twins of m. This form of m has been observed in peak-aged materials quenched into water and is thought to arise from a low temperature t $\rightarrow$ m tranformation [23]. Occasional large particles of twinned m were also present at grain boundaries and within the grain matrix. These particles contained coarse (0 0 1) twins and were the result of undissolved and unreacted pure ZrO_2 (Fig. 4a).

6.2. Effect of ageing on grain boundaries

As seen in the optical micrographs, the classical form of the decomposition occurred within the grain-boundary regions, as described earlier for Mg-CSZ. TEM observations of the decomposed grain-boundary regions in Mg-PSZ revealed a similar microstructure to that observed for the

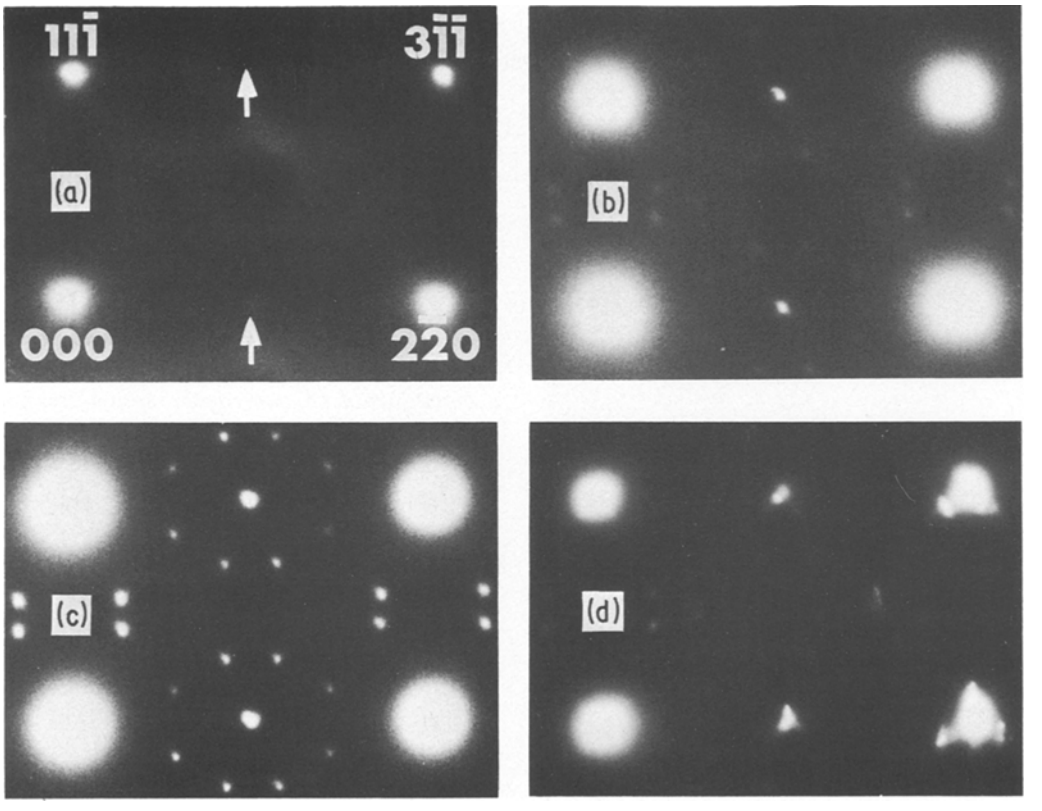

Figure 9 Sections of $[112]_c$ SAD patterns showing δ-phase development resulting from 1100° C ageing. (a) As-fired Mg-CSZ, (b) Mg-PSZ aged 0.5 h, (c) Mg-PSZ aged 2 h, and (d) Mg-PSZ aged 16 h. Indexed reflections are due to c-phase and arrowed spots are due to the t phase, respectively. All other reflections, in SADS (a), (b) and (c), are δ-phase reflections. In (d) intense m reflections are also present in addition to c-, t- and δ-phase.

CSZ material, differing only in that the MgO rich pipes were generally of a discontinuous nature. This discontinuous appearance is not unexpected considering that the overall MgO content was about 30% lower for the PSZ material.

6.3. Effect of ageing on grain interiors

Ageing the as-fired material for times as short as 0.5 h at 1100° C caused the appearance of additional sharp diffraction spots in the c/t SAD patterns. Within experimental error the t precipitate size remained constant for the duration of the ageing treatments performed in this study.

From [310] SAD sections the additional diffraction spots correspond closely to those expected from δ-phase [20] which has a composition of 28 mol% MgO. The series of [112] SAD pattern sections of Fig. 9a to d reflect the increase in size of the δ-phase domains from ~3 nm diameter to >10 nm diameter. Also, the m reflection intensities increase with increasing time. All SAD areas of Fig. 9 were obtained from matrix regions.

DF images produced by using δ-phase diffracted beams showed that the phase nucleated heterogeneously at the interface between the matrix and t precipitates. After ageing for 0.5 h at 1100° C the δ-phase boundary length was about 30 nm. Examination of such areas, in DF, using a t beam suggested that regions within a precipitate associated with δ-phase were sustaining considerable strain. Evidence for this strain is given by very localized bend contours which could be associated with the nucleated δ-phase (see Fig. 11b). Fig. 10 was obtained using a δ-phase reflection and shows the δ-phase (bright areas) in the matrix regions associated with the t precipitates (black regions).

When δ-phase or local MgO enrichment occurs in the interfacial regions, lattice strains resulting from a decrease in the c-lattice parameter are an accompanying feature. The maximum enrichment occurs for stoichiometric δ-phase, 28.57 mol%

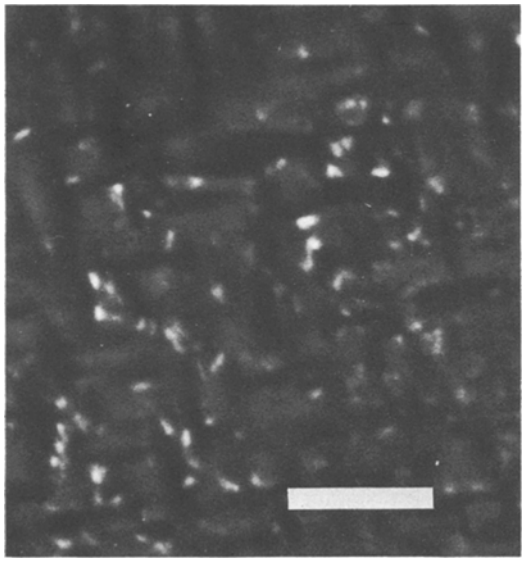

Figure 10 Mg-PSZ material aged 1 h, dark-field TEM image showing presence of δ-phase (bright areas) in c matrix regions between t precipitates (very dark areas). Two diffracted δ-phase beams were used to form image. Bar length equals 0.25 μm.

MgO, the unit cell volume of which corresponds to 7/4 cells of c-phase with $a_0 = 5.049$ Å [19]. An indication of the change in strain or misfit parameter of the interfacial region, resulting from the δ-phase, is readily obtained from the Brooks relationship [21], used in a previous study [10]. In this study the maximum coherent boundary length for a_0 of the c-phase with the c-axis of the t-phase was determined to estimate the maximum t precipitate size prior to m tranformation. By substituting into the relationship the values for c-phase a_0 and t-phase c, from Table I, and the equivalent δ-phase a_0, we obtain a coherent boundary length of about 25 nm for the c-phase/t-phase c-axis interface and about 20 nm for the δ-phase/t-phase c-axis interface. This form of analysis gives a useful indication of the magnitude and direction of the variation in coherent boundary length, resulting from the presence of the δ-phase (see Appendix). The consequences of this change on the mechanical properties will be discussed in Section 6.4.

Additional experiments have shown that for large δ-phase domains (Fig. 9c) to form, the t precipitates must have their longest dimension exceeding about 50 nm. Support for this observation comes from a number of sources. Mg-PSZ material prepared for an earlier investigation [10] and containing precipitates of t about 50 nm in size, could be induced to develop large δ-phase domains when annealed for 2 h at 1000° C. By contrast, the CSZ containing precipitates to about 50 nm could no be induced to develop large δ-phase particles after annealing times up to 4 h. Furthermore, Porter and Heuer [12] aged an 8.1 mol% MgO–ZrO_2 containing 5 nm precipitates of t at various sub-eutectoid temperatures and did not report any extra phases. Porter [24], however, independently reported that the 8.1 mol% MgO–ZrO_2 material of [12] contained micro-domains of an ordered phase, which did not increase in size as a consequence of subsequent ageing treatments.

These observations suggest a number of necessary conditions for the development and growth of the δ-phase. Firstly, nucleation of δ-phase can only occur when the solute content of the matrix is locally high enough. In as-fired and rapidly cooled PSZ materials it is reasonable to assume that complete precipitation (to the equilibrium volume phase content) of "pure" t ZrO_2 has not occurred. Therefore the matrix regions will not have attained the eutectoid composition and the precipitates of t probably contain a composition gradient with respect to their equilibrium composition. Studies of these materials have been published elsewhere [10, 12, 24]. The possibility of a composition/size dependence for t has been discussed by Heuer (in [1]), and was also suggested by the observations of the CSZ material where the t-phase was not detected even after 2 h ageing. Earlier work [10, 27], also using X-ray measurements, have shown that in materials containing very small t particles, the t c-axis varies markedly with composition fluctuations and that the c/a ratio does not attain the equilibrium value. Secondly, nucleation of the δ-phase is heterogeneous and so require a nucleation site, in this case the interface between the matrix and t precipitate. Thirdly, this interface must be large enough (i.e. sufficiently strained) so that lattice dilation facilities initiate "easy" growth of the phase. The last point immediately suggests that the t precipitates must be of a size where they contain at least a core of pure t ZrO_2 as this will ensure maximum c/t mismatch. It also suggests that the equilibrium t-phase content has precipitated, so that any further diffusion of Mg ions to the matrix–precipitate interface causes hyper-eutectoid enrichment of the matrix. It should be stated that the occurrence of large δ-phase domains is peculiar to sub-eutectoid ageing temperatures,

perhaps because the phase is a metastable form of the decomposition reaction. The X-ray measurements have not supported such local enrichment. However, the total volume of the regions may be too small to be detected by X-ray measurements [28].

Ageing for times between 2 and 4 h introduced thermal up-shock resistance. During this time the microstructure underwent a further distinct change. The initial localized highly strained regions within the t precipitates now exhibited a distinct diffraction contrast in the form of "mottling" (Fig. 11c). SAD patterns from these regions showed increased m diffraction intensity (see Fig. 9d). The DF image of Fig. 11c is interpreted in terms of t precipitates with m inter-growths (mottled regions). Examination of a number of foils revealed that the discrete *m* regions were also associated with δ-phase in the matrix.

Another feature in the foils of samples heat treated for 2 to 4 h, was that in some regions, former t precipitates had completely transformed to the room temperature stable m form. Measurements of the longest dimension of these precipitates suggested that whilst they were slightly larger than average they had not grown significantly and so had most likely transformed to m, at temperature or on cooling, owing to the interfacial strains. These precipitates have been described as Type 3 in another study [16] and are thought to be primarily responsible for the enhanced thermal up-shock resistance. This very fine dispersion of "microcrystalline" m as discreet intergrowths and Type 3 precipitates is referred to as grain matrix monoclinic (gmm); its presence is required for thermal up-shock resistance as will be discussed further in the next section.

In a different set of samples [16], thermal up-shock resistance was not achieved until ageing times of about 10 h at 1100° C. This material differed from the samples described here only in that there was no calcination step before final fabrication and firing. The microstructure in the interior of the grain in this sample showed the same features and development as the material described in the present work. Therefore, various batches of nominally the same composition and heat treatment may require different ageing times, i.e. incubation periods, to achieve the required increase of gmm for optimum properties.

At ageing times beyond 4 h, for the current batch, the fraction of gmm also increased. The size distribution of the m-phase contributing to the gmm content was still only marginally larger than the previously measured average t-phase size distribution. An interesting feature was that the distribution of the transformed gmm was very inhomogeneous. For example, within the same grain, one area would show t precipitates with strain contours (with SAD pattern of c-, t- and δ-phase) whilst in an adjacent area the precipitates had transformed to m. This type of inhomogeneous phase distribution was present in all samples, up to the maximum ageing time of 32 h.

Up to the maximum ageing time studied, the only features observed in the grain interior were those described above. To this extent the "classical" eutectoid decomposition also did not occur in a matrix containing a significant amount of t-phase, and like the CSZ material was restricted to grain-boundary nucleation and growth. If, as has been suggested earlier, the nucleation and growth of the δ-phase was a form of decomposition reaction occurring within the grain matrix, then the decomposition reaction was incomplete, because the Mg-ion segregation did not proceed beyond the δ-phase composition 28 mol % MgO.

6.4. Role of microstructure on mechanical properties

At the shortest ageing times, the formation of large δ-phase particles causes an enhancement of the room-temperature MOR. As described previously, this enhancement was achieved by destabilizing and so increasing the t particle size range, i.e. smaller t precipitates became available for transformation in the stress field of a propagating crack. As discussed earlier it is the change in interfacial misfit coupled with a possible change in the chemical composition, resulting from MgO diffusion out of the t-phase, which is responsible for the destabilization of the t-precipitates. From Fig. 2 it can be seen that the MOR increase is maximized at 2 h. Beyond 2 h the GB m and the increase in gmm begin to show a small but definite effect on the MOR.

The Mg-PSZ studied in this work acquires thermal up-shock resistance after ageing for 1 h at 1100° C. We attribute this enhancement to the ever increasing presence of the two forms of gmm. From empirical measurements, predominantly by X-ray techniques [16, 29], it was determined that optimum thermal up-shock properties were obtained with a gmm generally about 10% by

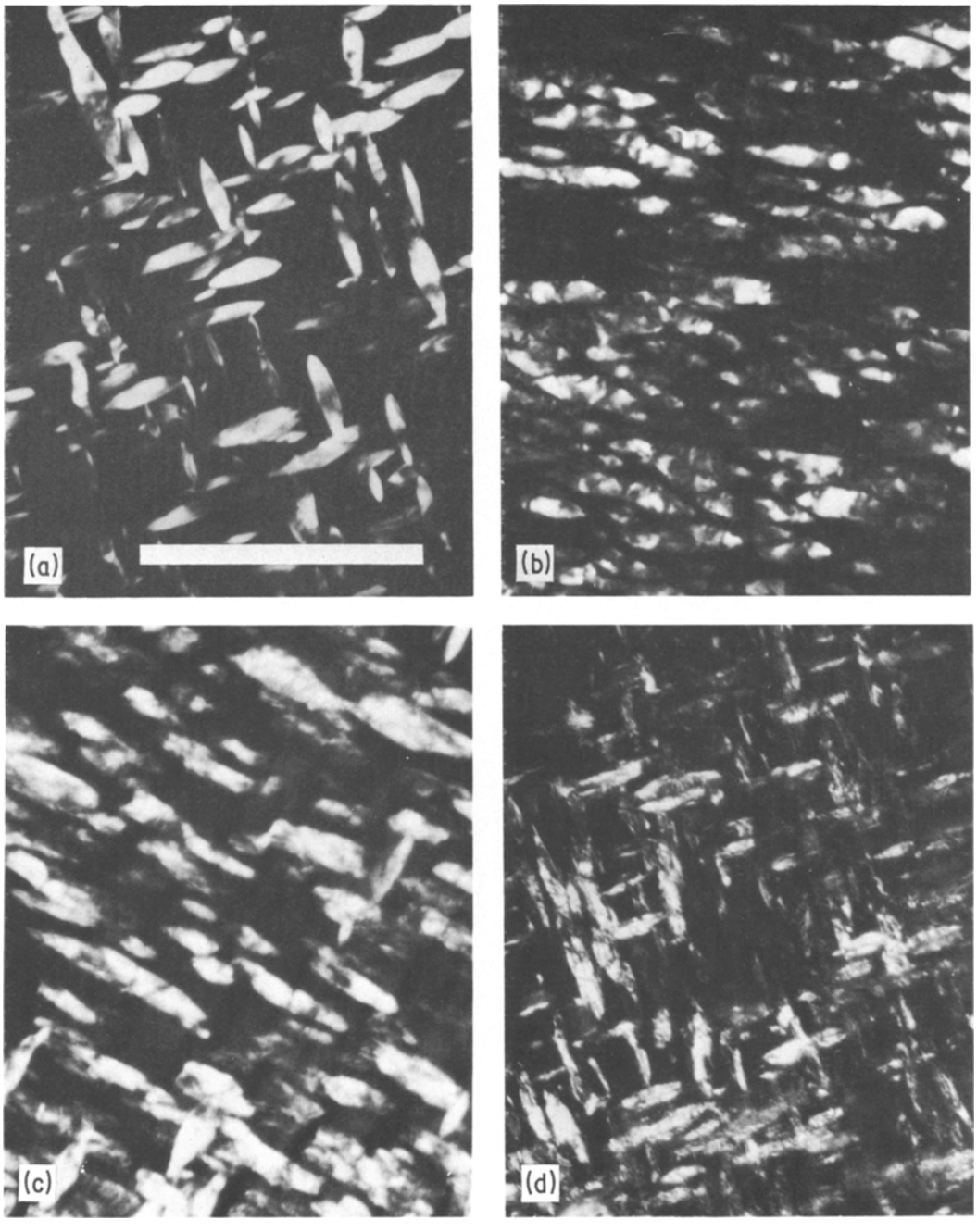

Figure 11 Series of dark-field TEM images showing effect of 1100° C ageing on t precipitates in Mg-PSZ. (a) As-fired material, electron beam close to [001]. (b) Highly strained regions within t precipitates at equivalent of 0.5 h ageing, electron beam close to $[2\bar{1}5]$. (c) Strained t and "mottled" regions due to m intergrowths in t precipitates after 2 h ageing, electron beam close to $[2\bar{1}9]$. (d) t precipitates with m intergrowths and twinned m precipitates (Type 3, [15]) transformed on cooling, electron beam close to [103]. Bar length equals 0.5 μm, all images at same magnification.

volume precipitate content and a GB m content of less than 5%.

The 2 h sample in the present batch has approximately these contents. In such materials the thermal up-shock resistance is explained on the basis of two physical phenomena. Firstly, some of the very fine m precipitates transform back to t over a large temperature range, 450 to 900° C rather than at the $m \rightarrow t$ equilibrium phase-diagram boundary-temperature of ~ 1200° C [9], thereby

counteracting some of thermal expansion strains due to the temperature increase. Secondly, the presence of the very fine m precipitates enhances the fracture toughness with an increased R-curve behaviour [17].

For ageing times in excess of 2 h the grain-boundary phase exerts an increasing influence on the fracture properties. The gmm was also still increasing and up to the maximum time examined, 32 h, had increased to about 30%. It would be anticipated that if the GB m-phase could be suppressed, Mg-PSZ with about 30% by volume gmm would show extremely good thermal up-shock resistance.

7. Summary and conclusions

In CSZ, 14 mol% MgO–ZrO_2, decompositon due to ageing at 1100° C proceeded at grain boundaries and pores via the reaction predicted from the phase diagram, namely, CSZ decomposed to m ZrO_2 plus an MgO rich phase. Within the grains a t-phase was homogeneously nucleated as small discs, which grew on $\{100\}_c$. Also within the grains the δ-phase, was formed. This phase was present as micro-domains, ~ 3 nm diameter, until the c completely decomposed (after 6 h at 1100° C). The overall decomposition rate was similar to that reported by Viechnicky and Stubican [13] for a 20 mol% MgO–ZrO_2 alloy. The loss in strength between 2 and 6 h ageing at 1100° C is attributed to the cracking which occurred as a result of the thermal expansion differences between the c- and m-phases. Thermal up-shock resistance was achieved when the fine grained, microcrack-laden m-phase became dominant in the microstructure.

The decomposition rate of a PSZ, 9 mol% MgO–ZrO_2 alloy, aged at 1100° C was about an order of magnitude slower than that of the CSZ. Whilst the equilibrium decomposition products were also nucleated at grain boundaries their growth was retarded because of the lower solute content of the matrix and to a lesser extent by the precipitates within the matrix. Within the c/t interface the δ-phase nucleated and grew to > 10 nm diameter in the regions between the t precipitates. The chemical composition change associated with the growth of the δ-phase increased the matrix–precipitate misfit parameter and resulted in a severely strained interface between c and t. The added strain and increased misfit caused some of the t precipitates to acquire m intergrowths whilst other transformed to m on cooling to room temperature. At short ageing times, up to 4 h at 1100° C, the room-temperature mechanical properties were enhanced by the presence of the strained (destabilized) t and microcrystalline m precipitates. The increase in the matrix monoclinic content enhanced the thermal up-shock resistance and fracture toughness of the material. Beyond 4 h the decomposed grain-boundary phase reduced the strength until at about 32 h the mechanical properties were similar to those of the fully decomposed CSZ material.

Acknowledgements

The author thanks Messrs V. Gross and R. Hughan for providing the initial samples used in this work. The author also wishes to thank his colleagues for their comments and discussions, in particular M. J. Bannister, R. C. Garvie, H. R. Rossell and H. G. Scott.

Appendix

The one-dimensional (i.e. boundary length) Brooks' analysis may be criticized on the basis that it is inadequate and a more rigorous three-dimensional (i.e. particule radius) approach, such as proposed by Brown *et al.* [25, 26], is more appropriate when considering precipitates. There are a number of reasons why the results obtained by the simple approach are still useful and relevant when determining interfacial coherency limits.

(a) Previously [10], the Brooks' criterion consistently has yielded calculated coherency limits within a factor of 2 of those measured for the c/t interface in MgO-PSZ and CaO-PSZ. Since the formula yields an underestimate in most cases [21] the agreement obtained appears excellent. The experimentally observed values of critical radius determined by Brown *et al.* are also low by a factor of 2 or 4, depending on the nature of the interface [25, 26].

(b) In the Mg-PSZ system here, we are concerned with ellipsoidal or lenticular t precipitates which grow with $c//a$ of c-phase, so that only the magnitude of the c-axis controls the coherency limits (ref. Table I). By contrast, Brown *et al.* consider spherical precipitates of a "vacancy" type.

(c) In the present work we set out to determine what effect, if any, the presence of the δ-phase has on the coherent interfacial boundary

length. Since we are concerned only with the t *c*-axis the one-dimensional approach is valid as it will give an indication of the direction of the change.

The only valid criticism which can be made is in the selection of the Burgers vector of the interfacial dislocation. This critism could equally be true for the three-dimensional approach.

References

1. "Science and Technology of Zirconia", Advances in Ceramics, Vol. 3 edited by A. H. Heuer and L. W. Hobbs (The American Ceramic Society, Columbus, Ohio, 1981).
2. R. C. GARVIE, R. H. J. HANNINK and R. T. PASCOE, *Nature* **258** (1975) 703.
3. D. L. PORTER and A. H. HEUER, *J. Amer. Ceram. Soc.* **60** (1977) 183.
4. M. V. SWAIN, R. H. J. HANNINK and R. C. GARVIE, Symposium on the Fracture Mechanics of Ceramics, Pennsylvania State University, July 1981, Vols. 5 and 6 (Plenum Press, New York) to be published.
5. N. CLAUSSEN and M. RUHLE, in "Science and Technology of Zirconia", Advances in Ceramics, Vol. 3 edited by A. H. Heuer and L. W. Hobbs (The American Ceramic Society, Columbus, Ohio, 1981).
6. F. F. LANGE, ONR Technical Report No. 7, Contract N 00014-77-C-0441, May (1979).
7. K. G. BANSAL and A. H. HEUER, *J. Amer. Ceram. Soc.* **58** (1975) 235.
8. R. T. PASCOE, R. H. J. HANNINK and R. C. GARVIE, *Sci. Ceram.* **9** (1977) 447.
9. C. F. GRAIN, *J. Amer. Ceram. Soc.* **50** (1967) 288.
10. R. H. J. HANNINK, *J. Mater. Sci.* **13** (1978) 2487.
11. E. RYSHKEWITCH, "Oxide Ceramics" (Academic Press, New York, 1970) p. 358.
12. D. L. PORTER and A. H. HEUER, *J. Amer. Ceram. Soc.* **62** (1979) 298.
13. D. VIECHNICKI and V. S. STUBICAN, *ibid.* **48** (1965) 292.
14. B. YA. SUKHAREVSKII, A. M. GAVRISH and E. I. ZOZ, *Inorg. Mater.* **11** (1975) 393.
15. R. C. GARVIE, R. H. J. HANNINK and N. A. MCKINNON, US Patent No. 4 279 655 (1981).
16. R. H. J. HANNINK and R. C. GARVIE, *J. Mater. Sci.* **17** (1982) 2637.
17. M. V. SWAIN, Symposium on the Fracture Mechanics of Ceramics, Pennsylvania State University, July 1981, Vols. 5 and 6 (Plenum Press, New York) to be published.
18. M. V. SWAIN, R. C. GARVIE and R. H. J. HANNINK, *J. Amer. Ceram. Soc.* (1982) in press.
19. H. G. SCOTT, unpublished results.
20. R. H. J. HANNINK and H. J. ROSSELL, *Micron* **11** Suppl. 1 (1980) 36 (abs).
21. P. B. HIRCH, A. HOWIE, R. B. NICHOLSON, D. W. PASHLEY and M. J. WHELAN, "Electron Microscopy of Thin Crystals" (Butterworths, London, 1965) Ch. 14.
22. W. J. CAMBELL and C. F. GRAIN, US Bur. Mines RI 5982 (1962).
23. L. H. SCHOENLEIN, MSc thesis, Case Western Reserve University (1979).
24. D. L. PORTER, PhD thesis, Case Western Reserve University, (1977).
25. L. M. BROWN, G. R. WOOLHOUSE and G. VALDRÉ, *Phil. Mag.* **17** (1968) 781.
26. L. M. BROWN and G. R. WOOLHOUSE, *ibid.* **21** (1970) 329.
27. R. H. J. HANNINK, unpublished results (1978).
28. H. J. ROSSELL, private communication (1981).
29. CSIRO, unpublished results (1979).

Received 28 June
and accepted 12 July 1982